Zierenberg, R.A., Fouquet, Y., Miller, D.J., and Normark, W.R. (Eds.)
Proceedings of the Ocean Drilling Program, Scientific Results Volume 169

4. $^{230}Th/^{234}U$ and $^{231}Pa/^{235}U$ Disequilibria in Massive Sulfides from the Bent Hill Area (Legs 139 and 169)[1]

J.C. Scholten,[2] K.S. Lackschewitz,[2] V. Marchig,[3] P. Stoffers,[2] and A. Mangini[4]

ABSTRACT

Massive sulfide samples from the Bent Hill area were analyzed for $^{230}Th/^{234}U$ and $^{231}Pa/^{235}U$ disequilibria. Apparent ages calculated from these ratios are between 8.2 and >300 ka. Concordant ages were found for only three samples that originate near the surface from the clastic sulfide zone and suggest "true" ages of between 8.5 and 16.0 ka (mean of ^{230}Th and ^{231}Pa ages). The uranium vs. depth distribution in the Bent Hill Massive Sulfide deposit suggests an open system for uranium for the deeper part of the deposit, which was probably caused by extensive recrystallization processes inhibiting true age determinations.

INTRODUCTION

The Bent Hill area, which is situated in the Middle Valley, northern Juan de Fuca Ridge, was the subject of detailed investigation during Ocean Drilling Program (ODP) Legs 139 and 169 (Fig. F1). A massive sulfide mound is located ~100 m south of the southern edge of Bent Hill (Bent Hill Massive Sulfide deposit, BHMS) (Fig. F2). A second mound of massive sulfide is present ~300 m further south (Ore Drilling Program Mound) (Fig. F2). Drilling during Leg 139 established that the BHMS deposit was formed by the discharge of hydrothermal fluids (350°–400°C) at the ocean floor; it also established that the metals

[1]Scholten, J.C., Lackschewitz, K.S., Marchig, V., Stoffers, P., and Mangini, A., 2000. $^{230}Th/^{234}U$ and $^{231}Pa/^{235}U$ disequilibria in massive sulfides from the Bent Hill area (Legs 139 and 169). *In* Zierenberg, R.A., Fouquet, Y., Miller, D.J., and Normark, W.R. (Eds.) *Proc. ODP, Sci. Results,* 169, 1–15 [Online]. Available from World Wide Web: <http://www-odp.tamu.edu/publications/169_SR/VOLUME/CHAPTERS/SR169_04.PDF>. [Cited YYYY-MM-DD]
[2]Institut für Geowissenschaften, Olshausenstrasse 40, 24118 Kiel, Federal Republic of Germany. **js@gpi.uni-kiel.de**
[3]Bundesanstalt für Geowissenschaften, Stilleweg 2, 30655 Hannover, Federal Republic of Germany.
[4]Akademie der Wissenschaften, Im Neuenheimer Feld 366, 69120 Heidelberg, Federal Republic of Germany.

Date of initial receipt: 1 March 1999
Date of acceptance: 3 November 1999
Date of publication: 30 June 2000
Ms 169SR-108

forming the massive sulfides were derived from leaching of a basaltic source (Davis, Mottl, Fisher, et al., 1992; Goodfellow and Peter, 1994; Peter et al., 1994). The lack of intercalations of sediments suggested a rapid formation of the sulfides. The BHMS was revisited during Leg 169 mainly for the purpose of assessing the thickness and the lateral extent of the mineralization. Various holes were drilled on north-south (Holes 1035A, 1035C, 1035F, 1035E, 1035H) and east-west (Holes 1035A, 1035D, 856H, 1035G) transects (Fig. F2). The sulfides recovered were subdivided into three sulfide zones consisting of clastic sulfides at the top, massive sulfides, and a sulfide feeder zone at the base (Fouquet, Zierenberg, Miller, et al., 1998). The clastic sulfides consist of sulfide breccia and rubble that derive from the top of the massive sulfide unit. The massive sulfide unit is characterized by a sulfide content >50%. Krasnov et al. (1994) distinguished five zones within the massive sulfide unit. The first zone is mainly composed of pyrite with minor amounts of sphalerite and magnetite. Pyrrhotite is the dominant mineral in the second zone, whereas the third zone is mainly composed of pyrite. The fourth zone consists of pyrrhotite with minor amounts of chalcopyrite. Based on geochemical data and mineralogical observations, Krasnov et al. (1994) suggested that secondary alteration and recrystallization significantly influenced the second and third zones.

Age dating of the massive sulfide deposits from the Bent Hill area on the basis of biostratigraphy proved to be difficult. Few investigations have been done on the Quaternary subarctic biostratigraphy in the Middle Valley area (Brunner, 1994), and calcareous material is poorly preserved in upper Pleistocene sediments because of the shallow calcite compensation depth during this time. Furthermore, fossils like diatoms, radiolarians, and calcareous nannofossils are found only rarely in hydrothermal deposits (Stakes and Franklin, 1994).

In recent years many successful investigations have been conducted to date hydrothermal deposits by using natural radionuclides of the U-Th decay chain as chronometers (Lalou et al., 1993; Lalou et al., 1985; Lalou and Brichet, 1987; Lalou et al., 1998). The disequilibria between $^{230}Th/^{234}U$ and $^{231}Pa/^{235}U$ can be utilized to date hydrothermal deposits covering time intervals of between 1,000–300,000 yr and 1,000–120,000 yr, respectively. There are, however, several assumptions to be made if $^{230}Th/^{234}U$ and $^{231}Pa/^{235}U$ disequilibria are to be used for dating purposes (Lalou and Brichet, 1987):

1. No exogenous ^{230}Th and ^{231}Pa should be incorporated into the deposits during and after their formation. Therefore, all the ^{230}Th and ^{231}Pa measured in the sample ought to come from the decay of authigenic ^{234}U and ^{235}U, respectively. An indication of the validity of this assumption would be the absence of ^{232}Th, which is generally of exogenous origin.
2. All the U measured in the sample must be coprecipitated with the deposit and no addition or loss of U may occur thereafter (closed system).

We have studied the $^{230}Th/^{234}U$ and $^{231}Pa/^{235}U$ disequilibria in massive sulfides obtained during Legs 139 and 169 from the BHMS and the Ore

F1. Location of the Middle Valley, p. 8.

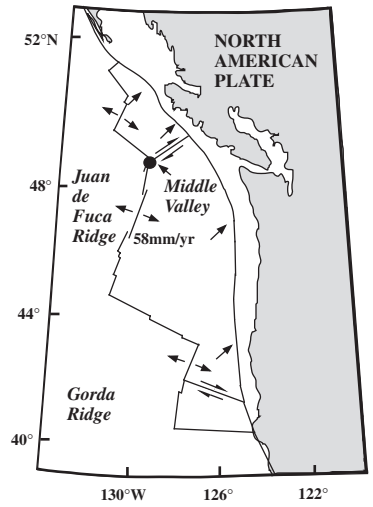

F2. Locations of the holes drilled during Legs 139 and 169, p. 9.

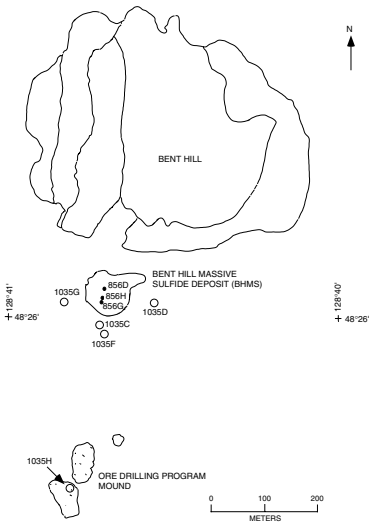

Drilling Program Mound to estimate the ages and history of massive sulfide formation in these areas.

METHODS

For the mineralogical and radiochemical analyses, one block of sample was crushed and ground. Identification of the mineralogical composition was performed by means of X-ray diffraction (XRD) analysis (Cu Kα). Thorium, uranium, and protactinium isotopes were determined by using ~0.5–1 g of the sulfide samples and adding a $^{228}Th/^{232}U$ and ^{233}Pa spike followed by chemical separation, as described by Anderson and Fleer (1982). ^{232}Th, ^{230}Th, ^{228}Th, ^{238}U, ^{234}U, ^{232}U, and ^{231}Pa were measured by alpha counting using a silicon surface detector. ^{233}Pa was measured by gamma counting using a germanium detector. Calibration of the spikes was performed with a UREM 11 certified reference ore. For some samples the purification procedure for uranium isotopes failed. These samples were reanalyzed for uranium and thorium isotopes. Duplicate and triplicate analyses of individual samples were also performed in order to check the reproducibility of radiochemical methods used. The results of XRD and radiochemical measurements are shown in Table T1.

T1. XRD and radionuclide analyses, p. 14.

Age Calculations

$^{230}Th/^{234}U$ ages were calculated by using the following equation given by Kaufmann and Broecker (1965):

$$^{230}Th/^{234}U = (^{238}U/^{234}U)[1 - \exp(-\lambda^{230}t)]$$

$$+ [1 - (^{238}U/^{234}U)][\lambda^{230}/(\lambda^{230}-\lambda^{234})][1 - \exp(\lambda^{234} - \lambda^{230})t], \quad (1)$$

where λ^{230} and λ^{234} are the decay constants of ^{230}Th and ^{234}U, respectively. The age t is calculated by iteration of Equation 1. $^{231}Pa/^{235}U$ ages were calculated by

$$t = -1/\lambda^{231} \cdot \ln[1 - (^{231}Pa/^{235}U)], \quad (2)$$

where λ^{231} is the decay constant of ^{231}Pa. ^{235}U was calculated from ^{238}U as follows:

$$^{235}U = ^{238}U/21.7, \quad (3)$$

where ^{238}U and ^{235}U are measured in decay units per minutes per gram.

RESULTS AND DISCUSSION

As indicated by Lalou et al. (1993), oxidation of massive sulfides may cause mobilization of uranium isotopes and, consequently, such material may not be useful for age determinations by means of $^{230}Th/^{234}U$ and $^{231}Pa/^{235}U$ disequilibria. In our study most of the samples consist of pyrite, pyrrhotite, and marcasite with trace amounts of magnetite, chalcopyrite, quartz, and barite (Table T1), and from these mineralogical re-

sults there are no indications that oxidized sulfides were analyzed. It was only in Sample 9 that goethite was found apart from marcasite. This sample was obtained from the CORK, which was deployed during Leg 139 (1991) and recovered during Leg 169 (1996). Age dating of these minerals within such a short time scale is not possible using the methods applied. ^{232}Th was detected in four samples (8, 13, 15, and 17). Whereas the uranium and thorium contents are relatively high in these samples, the effect of exogenous ^{230}Th and ^{231}Pa on the $^{230}Th/^{234}U$ and $^{231}Pa/^{235}U$ disequilibria is expected to be low.

Table T2 presents the data that were used to calculate the apparent $^{230}Th/^{234}U$ and $^{231}Pa/^{235}U$ ages using Equations 1 and 2. Average radionuclide activities were used for those samples where duplicate or triplicate analyses were performed. The apparent $^{230}Th/^{234}U$ and $^{231}Pa/^{235}U$ ages are between 8.2 and >300 ka and between 8.2 and >120 ka, respectively. The relation between both radionuclide ratios is shown in Figure F3. In the case of age concordance, the measured $^{230}Th/^{234}U$ and $^{231}Pa/^{235}U$ ratios of samples investigated should fall on the concordance line (solid line in Fig. F3). This concordance line was calculated for an initial $^{234}U/^{238}U$ ratio of 1.14, which is the ratio of seawater (Chen et al., 1986). Only Samples 1, 2, and 7 (within a 2-σ level) fall on this line and therefore their apparent $^{230}Th/^{234}U$ and $^{231}Pa/^{235}U$ ages can be regarded as "true" ages. This suggests a formation period between 8.5 and 16.0 ka (mean of ^{230}Th and ^{231}Pa ages) for the clastic sulfides at the top of the BHMS and the upper part of the massive sulfide zone (Fig. F4).

The large offset of the other ratios from the concordance curve may have several causes. One cause may be that the massive sulfides investigated are not a chemically closed system for ^{230}Th and ^{231}Pa and addition and/or loss of these isotopes may have occurred. Most investigations dealing with the behavior of thorium and protactinium in oceanic environments have shown that these elements are less soluble than uranium (Cochran, 1982). Therefore, discordant ratios are more likely to be caused by a chemically open system with respect to the gain and/or loss of uranium.

Most of the uranium in massive sulfides is believed to have a seawater origin (Lalou et al., 1993), because the $^{234}U/^{238}U$ ratio measured in most sulfides is similar to that of seawater ($^{234}U/^{238}U$ = 1.14). Relative to the uranium content in seawater (3.32 ppb) the hydrothermal fluids are poor in uranium (0.06–0.18 ppb) (Chen et al., 1986). Laboratory experiments indicated that in H_2S-bearing fluids the mobile form of uranium (U^{+6}) may be stable and no reduction was observed (Anderson et al., 1989; Kochenov et al., 1977). In the presence of mineral surfaces, however, there is a reduction of U^{+6} to less soluble U^{+4} and the uptake of uranium from the solution was found to be very effective (Wersin et al., 1994). Uranium is sorbed as finely dispersed uraninite minerals on the surface of the sulfide minerals (Wersin et al., 1994), which have a low solubility under chemically reducing conditions (Langmuir, 1978).

Massive sulfides precipitate because of cooling during mixing of hydrothermal fluids with seawater. Lalou et al. (1996) have shown that uranium uptake by sulfides occurs during and/or very soon after their formation and that the resulting uranium content is a function of local environmental conditions and thus very variable. As long as a reducing environment persists, uranium loss of the sulfides is expected to be minimal. Recrystallization of the sulfide minerals was observed in the Bent Hill deposits (Zierenberg et al., 1998; Krasnov et al., 1994) and large parts of the deposit have undergone changes because of continued cir-

T2. Radionuclide data used for age calculations, p. 15.

F3. $^{231}Pa/^{235}U$ vs. $^{230}Th/^{234}U$ ratios of samples investigated, p. 10.

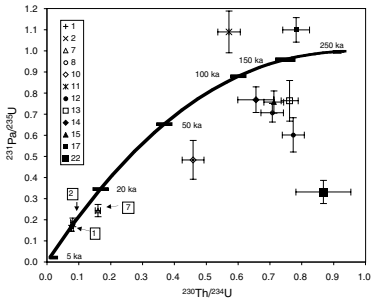

F4. North-south section across the BHMS deposit, p. 11.

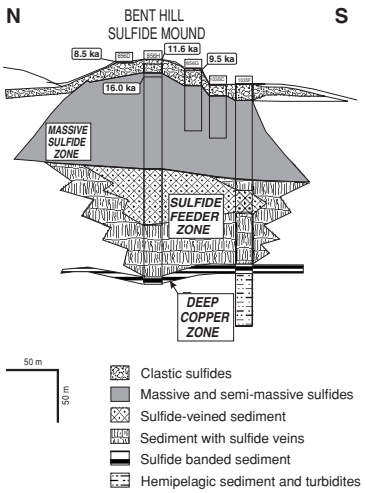

culation of hydrothermal fluids and seawater through the sulfide mound after initial deposition of the sulfide (Marchig and Dietrich, 1996). Such processes are likely to affect the uranium concentrations of the sulfides.

The $^{234}U/^{238}U$ ratios in the samples investigated are within the analytical uncertainties in the same range as that of seawater ($^{234}U/^{238}U$ = 1.14). If there was a closed system for uranium in the samples investigated, all ratios measured should fall on the solid line in Figure F5, which indicates the change of the seawater ratios with time (i.e., $^{230}Th/^{234}U$). The effect of a recent loss of uranium (with $^{234}U/^{238}U$ = 1.14) is indicated by the broken line. As shown in Figure F5, it is not possible to decide within the analytical $^{234}U/^{238}U$ uncertainties whether individual samples have been a closed system for uranium or not.

There is remarkable change in uranium vs. depth distribution in the BHMS deposit (Fig. F6). Apart from two sulfide samples (15 and 17), which were derived from Hole 1035F, there is a decrease in the uranium concentrations of sulfides investigated with depth. All samples with concordant ages were sampled near the surface of the deposit and these samples also have high uranium concentrations. Therefore, it seems likely that a closed system of uranium exists only for sulfides deposited near the surface (e.g., Samples 1, 2, 6, and 7) and that in the deeper part recrystallization of the sulfide deposits resulted in an open system for uranium. In this case the true ages of the samples lying below the concordia curve (Fig. F3) are expected to be older than the calculated $^{230}Th/^{234}U$ and $^{231}Pa/^{235}U$ ages (^{231}Pa age < ^{230}Th age < true age), whereas for the two samples above the concordia curve the true ages should be younger than the calculated apparent ^{230}Th ages (Cheng et al., 1998).

ACKNOWLEDGMENTS

We gratefully acknowledge the assistance of the crews from Legs 139 and 169 and the ODP curator in providing samples for this research. We thank M. Arp for the laboratory analyses and J. Fietzke and N. Frank for the discussions on this research. We acknowledge the constructive reviews of C. Lalou, W. Moore, and R. Zierenberg that helped to improve the paper.

F5. $^{234}U/^{238}U$ ratios vs. $^{230}Th/^{234}U$, p. 12.

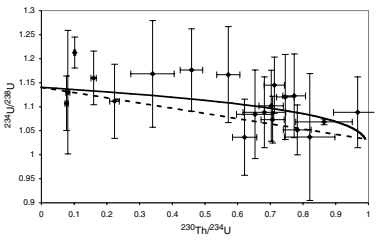

F6. ^{238}U vs. depth in samples investigated, p. 13.

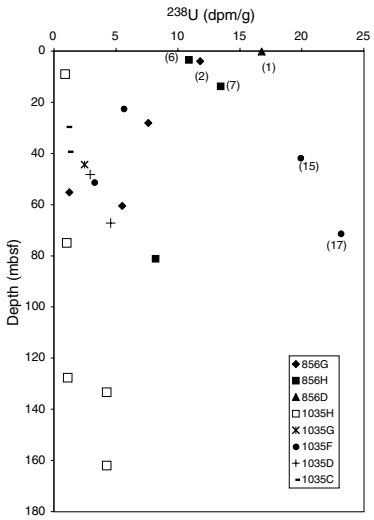

REFERENCES

Anderson, R.F., and Fleer, A.P., 1982. Determination of natural actinides and plutonium in marine particulate matter. *Anal. Chem.,* 54:1142–1147.

Anderson, R.F., Fleisher, M.Q., and Lehuray, A.P., 1989. Concentration, oxidation state and particulate flux of uranium in the Black Sea. *Geochim. Cosmochim. Acta,* 53:2215–2224.

Brunner, C.A., 1994. Planktonic foraminiferal biostratigraphy and paleoceanography of late Quaternary turbidite sequences at Holes 856A, 857A, and 857C, Leg 139. *In* Mottl, M.J., Davis, E.E., Fisher, A.T., and Slack, J.F. (Eds.), *Proc. ODP, Sci. Results,* 139: College Station, TX (Ocean Drilling Program), 39–58.

Chen, J.H., Wasserburg, G.J., von Damm, K.L., and Edmond, J.M., 1986. The U-Th-Pb systematics in hot springs on the East Pacific Rise at 21°N and Guaymas Basin. *Geochim. Cosmochim. Acta,* 50:2467–2479.

Cheng, H., Edwards, R.L., Murrell, M.T., and Benjamin, T.M., 1998. Uranium-thorium-protactinium dating systematics. *Geochim. Cosmochim. Acta,* 62:3437–3452.

Cochran, J.R., 1982. The oceanic chemistry of the U- and Th-series nuclides. *In* Ivanovich, M., and Harmon, R.S. (Eds.), *Uranium Series Disequilibrium: Application to Environmental Problems:* Oxford (Clarendon Press), 384–430.

Davis, E.E., Mottl, M.J., Fisher, A.T., et al., 1992. *Proc. ODP, Init. Repts.,* 139: College Station, TX (Ocean Drilling Program).

Fouquet, Y., Zierenberg, R.A., Miller, D.J., et al., 1998. *Proc. ODP, Init. Repts.,* 169: College Station, TX (Ocean Drilling Program).

Goodfellow, W.D., and Peter, J.M., 1994. Geochemistry of hydrothermally altered sediment, Middle Valley, northern Juan de Fuca Ridge. *In* Mottl, M.J., Davis, E.E., Fisher, A.T., and Slack, J.F. (Eds.), *Proc. ODP, Sci. Results,* 139: College Station, TX (Ocean Drilling Program), 207–289.

Kaufmann, A., and Broecker, W.S., 1965. Comparison of ^{230}Th and ^{14}C ages for carbonate material from Lake Lahontan and Bonneville. *J. Geophys. Res.,* 70:4039–4054.

Kochenov, A.V., Korolev, K.G., Dubinchuk, V.T., and Medvedev, Y.L., 1977. Experimental data on the conditions of precipitation of uranium from aqueous solutions. *Geochem. Int.,* 14:82–87.

Krasnov, S., Stepanova, T., and Stepanov, M., 1994. Chemical composition and formation of a massive sulfide deposit, Middle Valley, northern Juan de Fuca Ridge (Site 856). *In* Mottl, M.J., Davis, E.E., Fisher, A.T., and Slack, J.F. (Eds.), *Proc. ODP, Sci. Results,* 139: College Station, TX (Ocean Drilling Program), 353–372.

Lalou, C., and Brichet, E., 1987. On the isotopic chronology of submarine hydrothermal deposits. *Chem. Geol. (Isot. Geosci. Sec.),* 65:197–207.

Lalou, C., Brichet, E., and Hekinian, R., 1985. Age dating of sulfide deposits from axial and off-axial structures on the East Pacific near 12°50′N. *Earth Planet. Sci. Lett.,* 75:59–71.

Lalou, C., Reyss, J.L., and Brichet, E., 1993. Actinide-series disequilibrium as a tool to establish the chronology of deep-sea hydrothermal activity. *Geochim. Cosmochim. Acta,* 57:1221–1231.

————, 1998. Age of sub-bottom sulfide samples at the TAG active mound. *In* Herzig, P.M., Humphris, S.E., Miller, D.J., and Zierenberg, R.A. (Eds.), *Proc. ODP, Sci. Results,* 158: College Station, TX (Ocean Drilling Program), 111–117.

Lalou, C., Reyss, J.L., Brichet, E., Krasnov, S., Stepanova, T., Cherkashev, G., and Markov, V., 1996. Initial chronology of a recently discovered hydrothermal field at 14°45′N, Mid-Atlantic Ridge. *Earth Planet. Sci. Lett.,* 144:483–490.

Langmuir, D., 1978. Uranium solution-mineral equilibria at low temperatures with applications to sedimentary ore deposits. *Geochim. Cosmochim. Acta,* 37:547–569.

Marchig, V., and Dietrich, P.G., 1996. Hydrothermal activity in Middle Valley (Juan de Fuca Ridge 48°N): chemical redistribution between sediment, igneous rock and massive sulfides. *Sci. Drill.,* 5:267–281.

Peter, J.M., Goodfellow, W.D., and Leybourne, M.I., 1994. Fluid inclusion petrography and microthermometry of the Middle Valley hydrothermal system, northern Juan de Fuca Ridge. *In* Mottl, M.J., Davis, E.E., Fisher, A.T., and Slack, J.F. (Eds.), *Proc. ODP, Sci. Results,* 139: College Station, TX (Ocean Drilling Program), 411–428.

Stakes, D.S., and Franklin, J.M., 1994. Petrology of igneous rocks at Middle Valley, Juan de Fuca Ridge. *In* Mottl, M.J., Davis, E.E., Fisher, A.T., and Slack, J.F. (Eds.), *Proc. ODP, Sci. Results,* 139: College Station, TX (Ocean Drilling Program), 79–102.

Wersin, P., Hochella, M.F., Jr., Person, P., Redden, G., Leckie, J.O., and Harris, D.W., 1994. Interaction between aqueous uranium (VI) and sulfide minerals: spectroscopic evidence for sorption and reduction. *Geochim. Cosmochim. Acta,* 58:2829–2843.

Zierenberg, R.A., Fouquet, Y., Miller, D.J., Bahr, J.M., Baker, P.A., Bjerkgård, T., Brunner, C.A., Duckworth, R.C., Gable, R., Gieskes, J., Goodfellow, W.D., Gröschel-Becker, H., Guèrin, G., Ishibashi, J., Iturrino, G., James, R.H., Lackschewitz, K.S., Marquez, L.L., Nehlig, P., Peter, J.M., Rigsby, C.A., Schultheiss, P., Shanks, W.C., III, Simoneit, B.R.T., Summit, M., Teagle, D.A.H., Urbat, M., Zuffa, G.G., 1998. The deep structure of a sea-floor hydrothermal deposit. *Nature,* 392: 485–488.

Figure F1. Location of the Middle Valley at the Juan de Fuca Ridge.

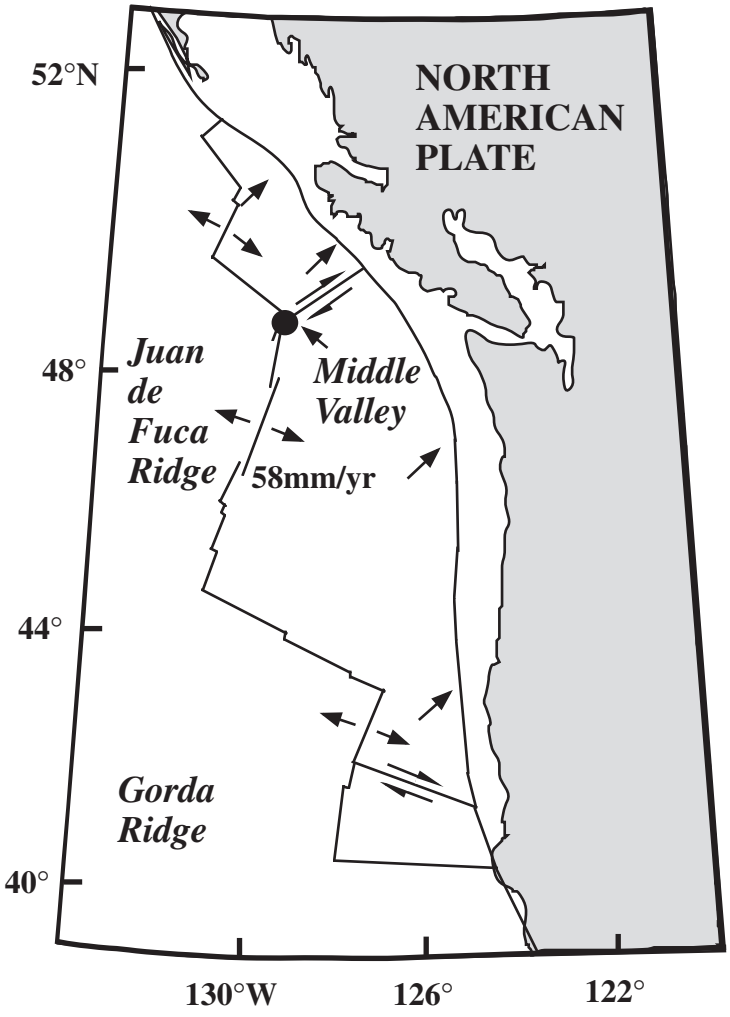

Figure F2. Locations of the holes drilled during Legs 139 (solid circles) and 169 (open circles) for which samples were available for this study.

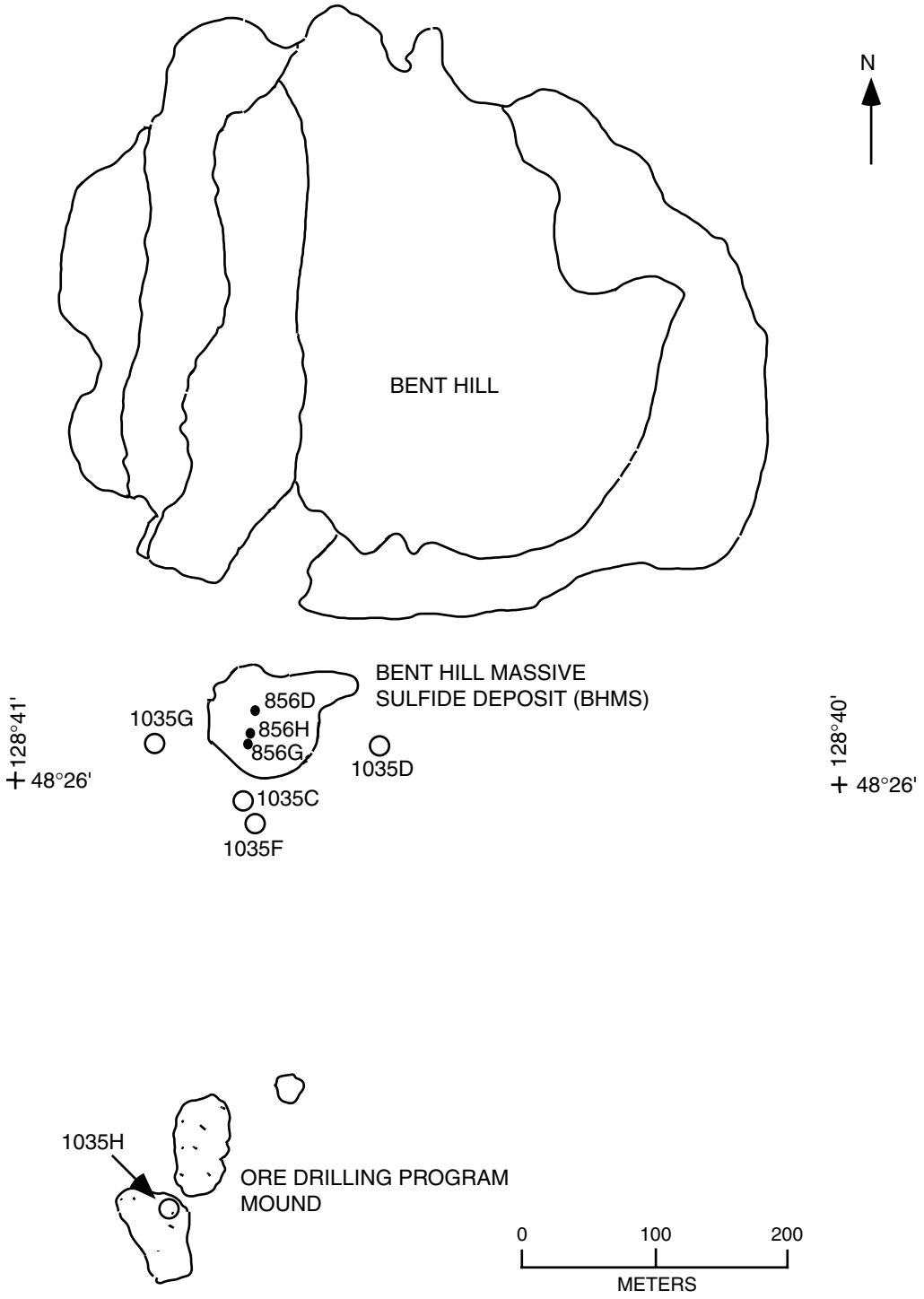

Figure F3. ^{231}Pa/^{235}U vs. ^{230}Th/^{234}U ratios of samples investigated. In the case of an age concordance, the ratios fall on the solid line; this concordia curve was calculated using Equations 1 and 2 with an initial ^{234}U/^{238}U = 1.14. Numbers in frames refer to sample number. Horizontal lines are isochrons and associated numbers indicate ages.

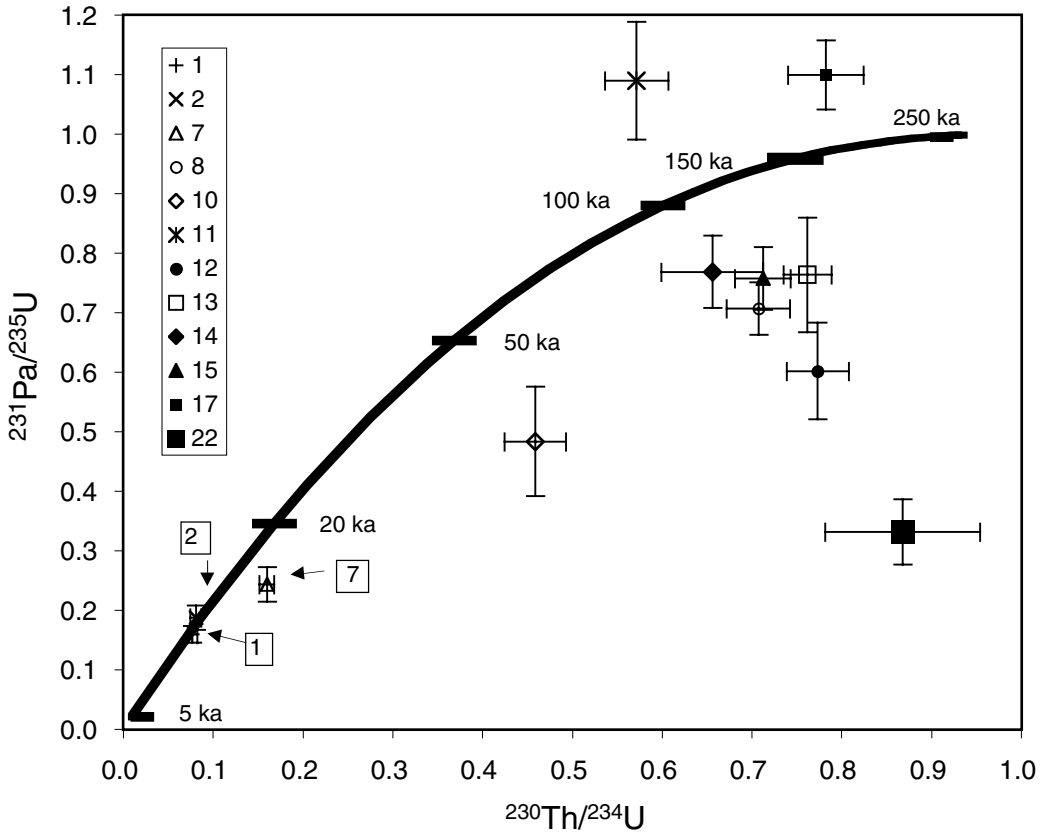

Figure F4. North-south section across the Bent Hill Massive Sulfide deposit. Apart from the age 11.6 ka (Sample 6), the ages shown were calculated using the mean of ^{230}Th/^{234}U and ^{231}Pa/^{235}U age models.

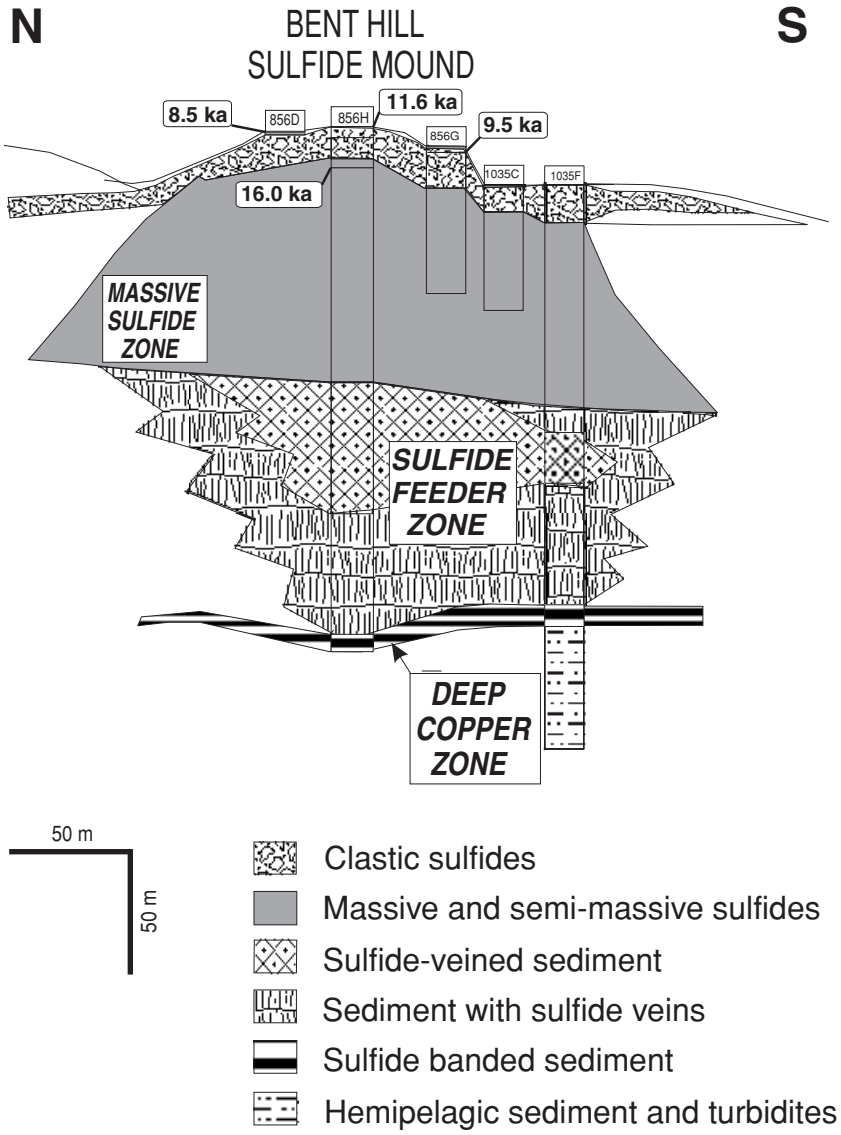

Figure F5. ^{234}U/^{238}U ratios vs. ^{230}Th/^{234}U. The solid line indicates the change of ^{234}U/^{238}U with time in the case of a closed system for uranium; the dashed line indicates the change of ^{234}U/^{238}U in the case of a recent loss of uranium (with ^{234}U/^{238}U = 1.14). Because of the analytical uncertainties, it is not possible to determine whether a closed system for uranium existed for the individual samples investigated or not.

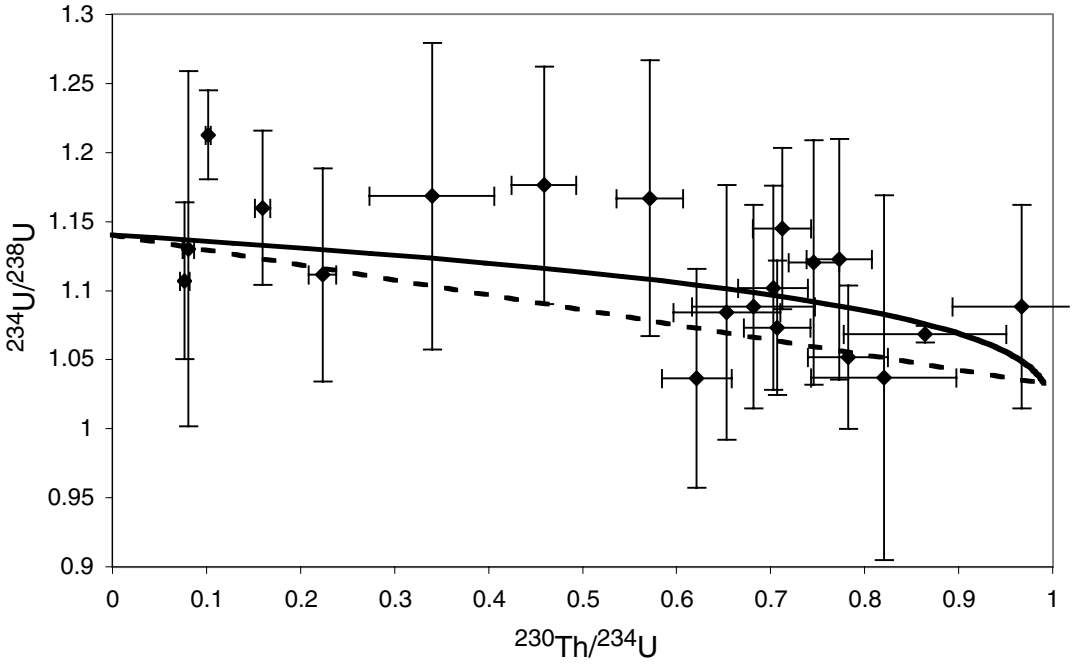

Figure F6. ^{238}U vs. depth in meters below seafloor (mbsf) in samples investigated. Apart from samples derived from Hole 1035F, there is a general decrease in ^{238}U concentration with depth. Concordant ages were calculated only for the samples from the upper part of the BHMS. Sample numbers are given in parentheses. Note that Hole 1035H is situated at Ore Drilling Program Mound.

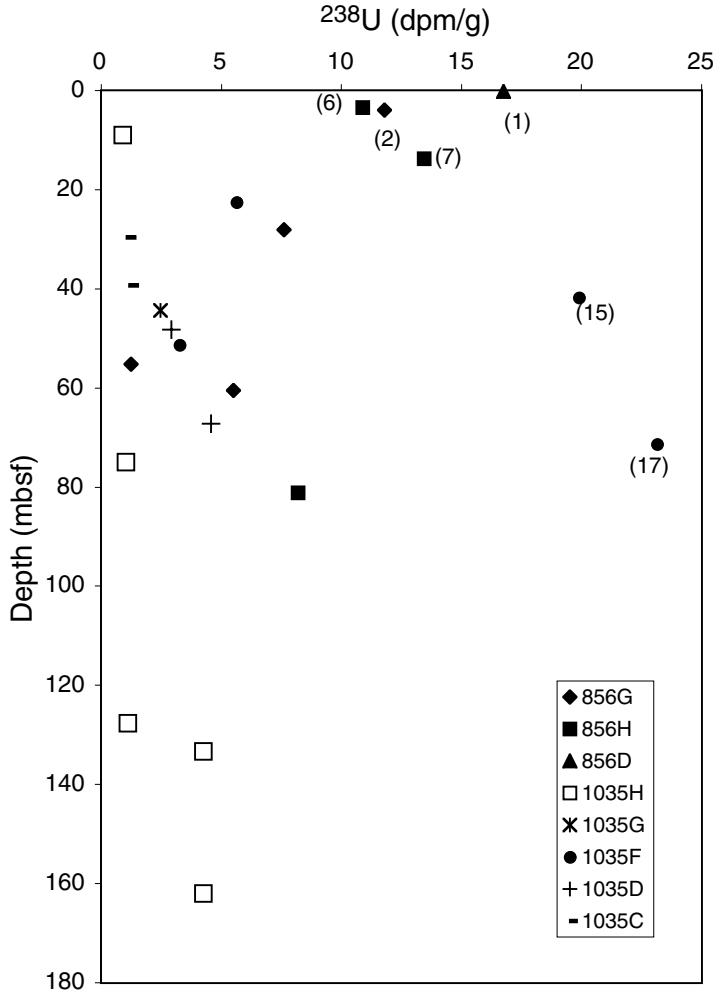

Table T1. Results of X-ray diffraction and radionuclide analyses.

Sample	Leg, hole, core, section, interval (cm)	Depth (mbsf)	Mineralogy	^{232}Th (dpm/g)	^{230}Th (dpm/g)	^{238}U (dpm/g)	^{234}U (dpm/g)	^{231}Pa (dpm/g)
1	139-856D-1H-1, 27-30	0.28	Py, M	ND	1.43 ± 0.07	16.8 ± 0.47	18.6 ± 0.80	0.123 ± 0.010
2	139-856G-1R-3, 94-96	3.95	Py, M	ND	1.08 ± 0.05	11.8 ± 0.29	13.4 ± 0.40	NA
				ND	1.09 ± 0.06	10.4 ± 0.26	11.9 ± 0.70	0.102 ± 0.007
3	139-856G-4R-1, 116-118	28.17	Py, Mg	ND	1.90 ± 0.07	7.63 ± 0.35	8.48 ± 0.44	NA
4	139-856G-6R-3, 41-43	55.30	Py	ND	0.80 ± 0.03	1.25 ± 0.08	1.29 ± 0.06	NA
5	139-856G-7R-4, 41-43	60.52	Py	ND	6.39 ± 0.30	5.52 ± 0.11	6.27 ± 0.20	NA
6	139-856H-1R-3, 51-57	3.54	Py	ND	1.34 ± 0.05	11.1 ± 0.20	12.7 ± 0.50	NA
				ND	1.36 ± 0.08	10.9 ± 0.19	13.2 ± 0.30	NA*
7	139-856H-2R-1, 36-38	13.87	Py, Mg	ND	2.50 ± 0.08	13.5 ± 0.38	15.6 ± 0.60	0.151 ± 0.018
8	139-856H-15R-1, 68-70	81.19	Pyr	0.082 ± 0.017	6.23 ± 0.22	8.21 ± 0.24	8.80 ± 0.31	0.267 ± 0.015
9	169-858G-17W-1, 79-80	0.79	Goe, M	ND	ND	NA*	NA*	NA
10	169-1035C-4X-1, 6-12	29.76	Py, M, Q	ND	0.58 ± 0.03	1.07 ± 0.06	1.26 ± 0.06	0.024 ± 0.004
11	169-1035C-5X-1, 6-19	39.40	M, Py	ND	0.76 ± 0.04	1.11 ± 0.06	1.31 ± 0.05	NA
				ND	0.80 ± 0.05	1.22 ± 0.08	1.41 ± 0.08	0.059 ± 0.003
12	169-1035D-7X-CC, 21-24	48.31	Py	ND	2.50 ± 0.14	2.83 ± 0.14	3.20 ± 0.16	NA
				ND	2.58 ± 0.13	3.03 ± 0.14	3.38 ± 0.14	0.081 ± 0.010
13	169-1035D-10X-1, 77-79	67.30	Py, M, Q	0.058 ± 0.013	3.91 ± 0.14	4.70 ± 0.26	5.20 ± 0.29	0.161 ± 0.012
				0.078 ± 0.014	3.75 ± 0.13	4.45 ± 0.24	5.06 ± 0.26	0.160 ± 0.011
14	169-1035F-3R-1, 5-6	22.55	Py, M	ND	4.01 ± 0.24	5.65 ± 0.33	6.13 ± 0.38	0.200 ± 0.011
15	169-1035F-5R-1, 6-7	41.8	Py, M, Q	ND	16.6 ± 0.64	20.7 ± 0.90	23.5 ± 1.00	NA
				ND	16.5 ± 0.72	20.1 ± 0.60	22.3 ± 1.10	0.695 ± 0.038
				0.148 ± 0.030	15.6 ± 0.40	19.0 ± 1.20	22.6 ± 1.30	NA*
16	169-1035F-6R-1, 1-3	51.41	Py, M, Mg, B	ND	2.59 ± 0.15	NA*	NA*	NA
				ND	2.50 ± 0.13	3.29 ± 0.16	3.62 ± 0.16	NA
17	169-1035F-8R-1, 75-77	71.35	Py, M	ND	18.6 ± 0.60	NA*	NA*	NA
				0.086 ± 0.011	19.5 ± 0.40	23.2 ± 0.57	24.4 ± 1.00	1.17 ± 0.055
18	169-1035G-2R-1, 4-6	44.44	Py, M	ND	3.24 ± 0.21	2.49 ± 0.16	3.12 ± 0.21	NA
19	169-1038H-1X-1, 10-12	0.10	Pyr	ND	ND	NA*	NA*	NA
				ND	ND	NA*	NA*	NA
20	169-1035H-2R-1, 26-29	9.06	Py, Ch, M	ND	0.41 ± 0.03	0.98 ± 0.05	1.19 ± 0.06	NA
					0.32 ± 0.02	0.92 ± 0.06	1.07 ± 0.06	NA
21	169-1035H-9R-1, 39-43	74.99	Py, M	ND	0.90 ± 0.04	1.05 ± 0.10	1.09 ± 0.09	NA
22	169-1035H-15R-1, 6-8	127.66	Pyr	ND	1.14 ± 0.05	NA*	NA*	NA
				ND	0.95 ± 0.05	1.11 ± 0.07	1.18 ± 0.06	0.017 ± 0.003
				ND	0.98 ± 0.04	1.11 ± 0.07	1.19 ± 0.06	NA*
23	169-1035H-16R-1, 74-77	133.34	Py, Pyr	ND	1.85 ± 0.07	1.95 ± 0.10	2.12 ± 0.11	NA
24	169-1035H-19R-1, 49-53	161.99	Py, Pyr	ND	4.50 ± 0.25	4.28 ± 0.19	4.65 ± 0.24	NA

Notes: Py = pyrite; M = marcasite; Mg = magnetite; Pyr = pyrrhotite; Goe = goethite; Q = quartz; B = barite; Ch = chalcopyrite. ND = not detected (under detection limit); NA = not analyzed; * = not analyzed because of a failure of the chemical purification procedure.

Table T2. Radionuclide data used for age calculations.

Sample	Leg, hole, core, section, interval (cm)	Depth (mbsf)	$^{234}U/^{238}U$	$^{230}Th/^{234}U$	$^{231}Pa/^{235}U$	Age (ka) $^{230}Th/^{234}U$	Age (ka) $^{231}Pa/^{235}U$
1	139-856D-1H-1, 27-30	0.28	1.11 ± 0.06	0.08 ± 0.01	0.16 ± 0.01	$8.6^{+0.8}_{-0.7}$	8.2 ± 0.7
2	139-856G-1R-3, 94-96	3.95	1.13 ± 0.13	0.08 ± 0.01	0.19 ± 0.02	$9.1^{+0.8}_{-0.7}$	9.8 ± 1.1
3	139-856G-4R-1, 116-118	28.17	1.11 ± 0.08	0.22 ± 0.01		$27.2^{+3.1}_{-2.6}$	
4	139-856G-6R-3, 41-43	55.30	1.04 ± 0.08	0.62 ± 0.04		$104.3^{+16.2}_{-131.0}$	
5	139-856G-7R-4, 41-43	60.52	1.14 ± 0.04	1.02 ± 0.06		>300	
6	139-856H-1R-3, 51-57	3.54	1.21 ± 0.03	0.10 ± 0.003		$11.6^{+0.4}_{-0.4}$	
7	139-856H-2R-1, 36-38	13.87	1.16 ± 0.06	0.16 ± 0.01	0.24 ± 0.03	$18.7^{+1.8}_{-1.4}$	13.2 ± 1.6
8	139-856H-15R-1, 68-70	81.19	1.07 ± 0.05	0.71 ± 0.04	0.71 ± 0.04	$130.0^{+20.0}_{-15.5}$	57.9 ± 3.6
10	169-1035C-4X-1, 6-12	29.76	1.18 ± 0.09	0.46 ± 0.03	0.48 ± 0.09	$65.2^{+10.1}_{-8.5}$	31.2 ± 5.9
11	169-1035C-5X-1, 6-19	39.40	1.17 ± 0.10	0.57 ± 0.04	1.09 ± 0.10	$89.5^{+12.5}_{-10.6}$	>120
12	169-1035D-7X-CC, 21-24	48.31	1.12 ± 0.09	0.77 ± 0.03	0.60 ± 0.08	$153.5^{+20.5}_{-17.0}$	43.5 ± 5.9
13	169-1035D-10X-1, 77-79	67.30	1.12 ± 0.09	0.75 ± 0.03	0.76 ± 0.10	$142.5^{+12.5}_{-11.3}$	67.6 ± 8.6
14	169-1035F-3R-1, 5-6	22.55	1.08 ± 0.09	0.65 ± 0.06	0.77 ± 0.06	$112.4^{+29.1}_{-20.4}$	68.9 ± 5.5
15	169-1035F-5R-1, 6-7	41.8	1.14 ± 0.06	0.71 ± 0.03	0.76 ± 0.05	$129.5^{+15.5}_{-13.0}$	66.9 ± 4.7
16	169-1035F-6R-1, 1-3	51.41	1.10 ± 0.07	0.70 ± 0.04		$127.5^{+19.5}_{-15.1}$	
17	169-1035F-8R-1, 75-77	71.35	1.05 ± 0.05	0.78 ± 0.04	1.10 ± 0.06	$161.0^{+36.0}_{-24.5}$	>120
18	169-1035G-2R-1, 4-6	44.44	1.25 ± 0.12	1.04 ± 0.10		>300	
20	169-1035H-2R-1, 26-29	9.06	1.17 ± 0.11	0.34 ± 0.07		$44.5^{+16.3}_{-12.4}$	
21	169-1035H-9R-1, 39-43	74.99	1.04 ± 0.13	0.82 ± 0.08		$182.0^{+92.0}_{-44.0}$	
22	169-1035H-15R-1, 6-8	127.66	1.07 ± 0.01	0.86 ± 0.09	0.33 ± 0.06	$206.0^{+95.0}_{-50.0}$	19.1 ± 3.2
23	169-1035H-16R-1, 74-77	133.34	1.09 ± 0.07	0.68 ± 0.07		$121.0^{+37.0}_{-24.5}$	
24	169-1035H-19R-1, 49-53	161.99	1.09 ± 0.07	0.97 ± 0.07		>300	

Note: In cases of duplicate and/or triplicate analyses of samples (Table **T1,** p. 14), the mean value with the standard deviation was used.